The potential for metal contamination during Apollo lunar sample curation

James M.D. Day[1*], Jennifer Maria-Benavides[1], Francis M. McCubbin[2], Ryan A. Zeigler[2]

[1]Scripps Institution of Oceanography, University of California San Diego, La Jolla, CA 92093

[2]NASA Johnson Space Center, Houston, Texas

Correspondence to: jmdday@ucsd.edu

Abstract words: 249

Main text: 3289

Figures: 4

Tables: 2, with three supplementary tables

31

32   **Abstract**

33   Curation and preparation of samples for chemical analysis can occasionally lead to significant

34   contamination. This issue is of concern in the study of lunar samples, especially those from the

35   Apollo sample collection, where available masses are finite. Here we present compositional data

36   for stainless steels that have commonly been used in the processing of Apollo lunar samples at

37   NASA Johnson Space Center, including a chisel and a vessel typically used to transfer Apollo

38   samples to principal investigators. The Type 304 stainless steels are Cr-rich, with high

39   concentrations of Mn (4000-18,000 $\mu g\ g^{-1}$), Cu (1000-22900 $\mu g\ g^{-1}$), Mo (1030-1120 $\mu g\ g^{-1}$) and

40   W (72-193 $\mu g\ g^{-1}$). They have elevated highly siderophile element concentrations (up to 92 ng g^{-1}

41   Os), $^{187}Os/^{188}Os$ ranging from 0.1310 to 0.1336, and negligible lithophile element abundances. We

42   find that, while metal contamination is possible, significant ($>>0.01\%$ by mass) addition of

43   stainless steel is required to strongly affect the composition of the highly siderophile elements

44   (HSE), W, Mo, Cr or Cu for most Apollo lunar samples. However, careful appraisal on a case-by-

45   case basis should take place to ensure contamination introduced through sample processing in the

46   curation labs is at acceptably low levels. A survey of lunar mare basalts and crustal rocks indicates

47   that metal contamination plays a negligible role in the compositional variability of the HSE and W

48   isotopes preserved in these samples. Further work to constrain contamination on other properties

49   of Apollo samples is required (e.g., organics, microbes, water, noble gases, magnetics), but the

50   effect of metal contamination can be relatively well-constrained for the Apollo lunar collection.

1. Introduction

Collection and return of planetary materials to Earth requires significant curational capability. In the first instance, as with the Apollo lunar samples, there is a basic requirement that samples are quarantined while tests are conducted for possible pathogens and hazards (Allton et al., 1998). For Apollo samples, early curation also included the requirement of handling samples under vacuum. Cabinets for sample handling and the tools used for sample subdivision were developed rapidly, and materials that could come into contact with pristine lunar samples were restricted to Type 304 stainless steel, series 6100 aluminum alloy, and Teflon™ (Allen et al., 2011). After the Apollo 17 mission, in 1972, the concept of handling samples under vacuum was abandoned. Apollo samples were moved, within the NASA Johnson Space Center to a new sample facility in Building 31, where they still reside and are handled in a dry N_2 atmosphere (Papanastassiou et al., 2015) with less than 10 ppm H_2O (Allen et al., 2011).

Numerous forms of potential contamination can affect Apollo samples during curation and sample processing and include – but are not limited to – exposure to magnetic fields, organics, anaerobic microbes, water, nitrogen, noble gases, lithophile elements (of special concern are those used for non-traditional stable isotope research), Pb and the moderately siderophile and highly siderophile elements, including Mo, W and Os (e.g., Pearce et al., 1974; Papanastassiou et al., 2015; Verchovsky et al., 2017). Extensive research has recently taken place on siderophile element abundances and isotopic compositions in lunar samples, which was previously not possible for these elements using the earlier methods of neutron activation analysis (NAA). Significant improvements in sensitivity using negative ion thermal ionization mass spectrometry (N-TIMS) and the advent of multi-collector inductively coupled plasma mass spectrometry (MC-ICP-MS) have enabled studies of: 1) tungsten isotopes to understand the timing and origin of lunar formation (e.g., Touboul et al., 2015; Kruijer et al., 2015); 2) Mo, Os isotopes and highly siderophile elements to examine the chemical signatures of impactors that struck the Moon after its initial differentiation (e.g., Puchtel et al., 2008; Fischer-Gödde & Becker, 2012; Burkhardt et al., 2014); and 3) investigation of late-accretion highly siderophile element signatures in the lunar interior and crust to understand metal-silicate and late accretion processes acting on the Moon (e.g., Day et al., 2016).

82   In this contribution, we provide the first report on the potential for curatorial contamination

83   during the handling of Apollo lunar samples, focused on the effect of metal contamination from

84   specific batches of Type 304 stainless steel that were used during the period over which much of

85   the recent HSE, W and Mo work on Apollo samples has occurred.

86

87   ## 2. Samples and Methods

88   We analyzed two metals that commonly come into direct contact with Apollo samples

89   during sample processing or transport. We analyzed a Type 304 stainless-steel fragment of a

90   chipping implement used for breaking fragments of lunar samples, and we took a fragment of a

91   standard stainless-steel container (9-6465), in this case used to ship a sample of the 'rusty rock'

92   sample 66095 used in a previous study (Day et al., 2017). Samples were prepared using a slow

93   speed, high-precision cutting diamond saw, and sawn surfaces were then sanded using corundum

94   paper and cleaned with distilled water. The stainless steels used for both objects are generally of

95   Type 304, but the major, minor, and trace element compositions of Type 304 stainless steel varies

96   substantially depending on the supplier and the raw materials used. To characterize the

97   composition of the metals, we undertook a systematic procedure of laser-ablation inductively

98   coupled plasma mass spectrometry (LA-ICP-MS), to document elemental variations in the metals

99   at <~0.1 mm scales and with limited total sample mass, and on larger mass aliquots by solution

100   ICP-MS, to obtain precise major and trace element concentrations, and isotope dilution

101   determination of highly siderophile elements, followed by N-TIMS analyses of Os isotopes. We

102   also characterized our in-house reference materials, the iron meteorites Hoba, Filomena and

103   Coahuila, to ensure accuracy, precision and consistency with prior work (e.g., Petaev & Jacobsen,

104   2004; Cook et al., 2004; Walker et al., 2008). All work was done at the Scripps Isotope

105   Geochemistry Laboratory.

106

107   Analysis by LA-ICP-MS was performed using a *New Wave Research UP213* (213 nm)

108   laser-ablation system coupled to a *ThermoScientific* iCAP Qc ICP-MS. Analyses were done using

109   ~0.5 mm long rasters with a 100 μm beam diameter, a laser repetition rate of 5 Hz, and a photon

110   fluence of ~3 to 3.5 J/cm^2. Ablation analysis took place in a 3 cm^3 ablation cell. The cell was

111   flushed with a He-gas flow to enhance production and transport of fine aerosols and was mixed

112   with an Ar carrier-gas flow of ~1 L/min before reaching the torch. Each analysis consisted of ~60

113   s data collection. Backgrounds on the sample gas were collected for ~20 s, followed by ~40 s of

114   laser ablation. Washout time between analyses was >120 s. Data were collected in time-resolved

115   mode so effects of inclusions, mineral zoning and possible penetration of the laser beam to

116   underlying phases could be evaluated. Plots of counts per second versus time were examined for

117   each analysis, and integration intervals for the gas background and the sample analysis were

118   selected. Standardization was performed using reference material iron meteorites Hoba, Coahuila

119   and Filomena, used by us and by other groups (e.g., McCoy et al., 2011).

120

121   Major- and trace-element abundances were determined using solution ICP-MS. Samples

122   and the reference material metal standards Hoba, Coahuila and Filomena were digested at 150°C

123   in Optima grade concentrated HF (4 mL) and HNO_3 (1 mL) for >72 hrs on a hotplate, with total

124   analytical blanks and standards. Samples were sequentially dried and taken up in concentrated

125   HNO_3 to remove fluorides, followed by dilution and doping with a 1 ppm indium solution to

126   monitor instrumental drift during analysis. Trace-element abundances were determined with a

127   *ThermoScientific iCAP* Qc quadropole ICP-MS in standard mode. Analyses were standardized

128   versus reference material BHVO-2 that was measured throughout the analytical run. In addition,

129   reference materials were analyzed as "unknowns" (BHVO-2, BIR-1, BCR-2, Hoba, Filomena,

130   Coahuila) to assess matrix matching, external reproducibility and accuracy. Special attention was

131   taken to circumvent the effect of potential interference from polyatomic species, and potential

132   interferences were monitored using the iron meteorite reference materials. For trace-elements,

133   reproducibility of the reference materials was generally better than 10% (RSD) and in line with

134   standard data measured in our laboratory (e.g., Day et al., 2017).

135

136   Osmium isotope and HSE abundance analyses were determined from metal aliquots that

137   were digested in sealed borosilicate Carius tubes, with isotopically enriched multi-element spikes

138   (^{99}Ru, ^{106}Pd, ^{185}Re, ^{190}Os, ^{191}Ir, ^{194}Pt), and 11 mL of a 1:2 mixture of multiply Teflon distilled HCl

139   and HNO_3 that was purged with H_2O_2 to remove Os. Samples were digested in Carius tubes to a

140   maximum temperature of 240°C in an oven for 72 hours. Osmium was triply extracted from the

141   acid using CCl_4 and then back-extracted into HBr, prior to purification by micro-distillation, with

142   the other HSE being recovered and purified from the residual solutions using anion exchange

143   separation (Day et al., 2016b). Isotopic compositions of Os were measured in negative-ion mode

144   on a *ThermoScientific* Triton thermal ionization mass spectrometer. Rhenium, Pd, Pt, Ru and Ir

145   were measured using an Cetac Aridus II desolvating nebulizer coupled to a *ThermoScientific* iCAP

146   Qc ICP-MS. Offline corrections for Os involved an oxide correction, an iterative fractionation

147   correction using $^{192}Os/^{188}Os$ = 3.08271, a ^{190}Os spike subtraction, and finally, an Os blank

148   subtraction. Precision for $^{187}Os/^{188}Os$, determined by repeated measurement of the UMCP

149   Johnson-Matthey standard was better than ±0.2% (2 St. Dev.; 0.11372 ±22; n = 9). Measured Re,

150   Ir, Pt, Pd and Ru isotopic ratios for sample solutions were corrected for mass fractionation using

151   the deviation of the standard average run on the day over the natural ratio for the element. External

152   reproducibility on HSE analyses using our method was better than 0.5% for 0.5 ppb solutions and

153   all reported values are blank corrected. The total procedural blanks (*n* = 2) run with the samples

154   had $^{187}Os/^{188}Os$ = 0.171 ± 0.003, with average quantities (in picograms) of 3.9 [Re], 73 [Pd], 2.5

155   [Pt], 11 [Ru], 2.5 [Ir] and 0.7 [Os]. All data are blank corrected, with the blanks representing

156   between less than 0.5% of Re, Pt, Ir and Os, less than 1.2% of Ru and less than 2% of Pd.

157

3. Results

159   The two metals that we analyzed are Type 304 austenitic stainless steels with between 75

160   to 82 wt.% Fe, 13.4 to 14.7 wt.% Cr and 4 to 8 wt.% Ni (**Table 1**, *Table S1*). The container steel

161   used for shipping is Mn-rich (1.9 wt.%), whereas the Type 304 stainless steel chipping implement

162   used for sample processing is Cu-rich (2.3 wt.%). Other notable elements with elevated

163   abundances include Co (480-1260 µg g^{-1}), Mo (1030-1120 µg g^{-1}), and high Nb in the chipping

164   implement (2600 µg g^{-1}). For the trace elements, concentrations of W, Zn, Ga, Se, Pb and Sn are

165   <200 µg g^{-1}, whereas the rare earth elements (REE) and large ion lithophile elements (LILE) are

166   <50 µg g^{-1}, or are at the limits of detection.

167

168   The highly siderophile elements (HSE: Os, Ir, Ru, Rh, Pt, Pd, Re, Au) were measured by

169   both LA-ICP-MS and isotope dilution methods (**Table 2**). The new isotope dilution HSE

170   abundances determined for the aliquots of Hoba, Coahuila and Filomena that we use for LA-ICP-

171   MS study agree well with previously reported values (Petaev & Jacobsen, 2004; Cook et al., 2004;

172   Walker et al., 2008; McCoy et al., 2011). For the austenitic stainless steels we find that results for

173   both isotope dilution and LA-ICP-MS are broadly similar, although the individual laser ablation

174   rasters for each sample (*n* = 4) indicate at least 20% variability in the distribution of the HSE within

175   the metals at <0.1 mm resolution is possible. The metals have elevated (10's ng g^{-1}) and

176   fractionated chondrite-normalized HSE patterns (**Figure 1**) and ^{187}Os/^{188}Os (0.1310-0.1336) ratios

177   that are above the chondritic range (0.126-0.128; Day et al., 2016).

178

179   **4. Discussion**

180   During any form of curation or preparation/processing of rock samples, there exists the

181   potential to contaminate. For example, contamination or modification of rocks can take place in

182   the form of interaction and modification by fluids, gases, or microbes, thermal processes that alter

183   the nature of the rock, such as sawing, or physical inclusion of foreign material by abrasion or

184   impact. For lunar samples curated at NASA Johnson Space Center, whether collected by astronauts

185   or collected as meteorites in Antarctica, these forms of modification are all possible. In the

186   discussion, we focus on the potential of these processes to modify the Apollo samples, although

187   many of the arguments applied here can equally be transplanted to understanding contamination

188   of meteorite samples. In so doing, we use evidence that obvious metal smearing has occurred on

189   the outside surfaces of at least some 1 to 2 g impact melt breccia fragments (Papanastassiou et al.,

190   2015) and during sawing (e.g., *Figure S8* of Tikoo et al., 2014), and that chipping implements with

191   brittle steels might lead to particulate contamination. The analyzed metals have negligible levels

192   of elements used in lithophile radiogenic and non-traditional stable isotope studies, like Sr (<0.45

193   μg g^{-1}), Nd (<0.024 μg g^{-1}), Hf (<0.16 μg g^{-1}), Pb (<3.35 μg g^{-1}), Rb (<0.68 μg g^{-1}), Zr (<3.5 μg g^{-1}

194    $^{-1}$), Zn (<19 μg g^{-1}), Ga (<25.3 μg g^{-1}), so we do not consider these elements further in the present

195   study.

196

197   *4.1 Potential for contamination of osmium and the highly siderophile elements*

198   A primary goal of this study is to define the effect of possible metal contamination on the

199   highly siderophile elements (HSE) due to curatorial processing at NASA Johnson Space Center.

200   The HSE have been particularly powerful tracers of late accretion to the Moon, including within

201   the lunar interior (e.g., Walker et al., 2004; Day et al., 2007; 2010; Day & Walker, 2015), as well

202   as within lunar impact breccias and melt-rocks (e.g., Higuchi and Morgan, 1975; Hertogen et al.,

203   1977; Korotev, 1994; Norman et al., 2002; Puchtel et al., 2008; Fischer-Gödde & Becker, 2012;

204   Sharp et al., 2014; Liu et al., 2015; Day et al., 2017; Gleißner & Becker, 2017). A persistent

205   concern is potential metal contamination during curation and curatorial sample processing, due to

206   the significant leverage of high HSE abundances (10's-100's ng g^{-1}) in the stainless steel tools

207   compared with pristine crustal rocks or mare basalts (0.001-0.1's ng g^{-1}), or impact melt rocks (1-

208   10's ng g^{-1}).

209

210   Previously, ^{187}Os/^{188}Os, a proxy for long-term Re/Os, and the relative and absolute

211   abundances of the HSE have been used as sensitive indicators to detect and constrain levels of

212   meteoritic contamination (Day et al., 2010). In addition to having highly elevated HSE

213   abundances, chondritic materials (as well as some iron meteorites) are characterized by limited

214   variations in the relative and absolute abundances of these elements (<40%; Horan et al., 2003;

215   Day et al., 2016). Osmium isotopic composition is especially diagnostic because the limited range

216   in Re/Os among chondrites and some irons leads to a restricted range in ^{187}Os/^{188}Os (e.g., Smoliar

217   et al., 1996; Horan et al., 2003). The diagnostic capability of Os isotopes assumes that magmatic

218   processes under most conditions should lead to rocks with non-chondritic relative HSE

219   abundances, including Re/Os. The ^{187}Os/^{188}Os of a truly pristine crustal sample should therefore

220   evolve away from a chondritic growth trajectory, even if it formed from a melt with chondritic

221   isotopic composition. This presumption is supported by (1) variably fractionated HSE abundances

222   for most mare basalts (Day & Walker, 2015), (2) data for terrestrial igneous rocks indicating highly

223   variable HSE partitioning characteristics (Day, 2013), and (3) distinctly non-chondritic ^{187}Os/^{188}Os

224   and relative HSE abundances in some lunar crustal rocks (Day et al., 2010). Lunar non-mare

225   samples with chondritic or near-chondritic ^{187}Os/^{188}Os and relative HSE abundances are presumed

226   to have HSE dominated by one or more exogenous component(s).

227

228   Using the same logic, taking the composition of the Type 304 chipping implement stainless

229   steel as contaminant yields a mixing curve that begins at a factor of ~5 to 7 times less Os

230   concentration and more radiogenic ^{187}Os/^{188}Os compared with a chondritic impactor contaminant

231   (**Figure 2**). The curve for the stainless steels does not pass through the main cluster of pristine

232   crustal rocks or mare basalts, but does pass through the most radiogenic ^{187}Os/^{188}Os for some lunar

233   impact melt breccias. However, to account for the Os isotope composition of these rocks would

234   require between 1 to 100% by mass contamination by the stainless steel implements, which is far

235   in excess of any realistic contamination levels. Critically, the strongly fractionated HSE pattern of

236   the steels (**Figure 1**) would, in turn, strongly impact the HSE patterns of lunar samples that, to

237   date, has not been observed. For example, contamination by stainless steel would lead to equal

238   effects on all the HSE. The metals have Os/Ir of 3.3 ±1.9 and Ru/Ir = 4.2 ±2.4, but no mare basalt

239   (Os/Ir = 1.4 ±0.8; Ru/Ir = 3.1 ±2.9 [Day & Walker, 2015]), or lunar crustal rock (Os/Ir = 0.8 ±0.4;

240   Ru/Ir = 3.7 ±2.7 [Day et al., 2010]) has Os/Ir and Ru/Ir characteristics that match this signature.

241   While mixing curves in **Figure 3** might be taken to imply contamination of 0.001 to 0.1% of

242   stainless steel from curatorial processing to affect the Os isotopic composition of some mare

243   basalts and lunar pristine crustal rocks, the collateral effects on Os/Ir or Ru/Ir would be severe and

244   detectable. Our results imply that, while metal contamination can affect some lunar rocks during

245   curatorial processing, the potential for impact on the HSE abundances of samples is low.

246

247   ### *4.2 Potential for contamination of W, Mo, Cr and highly chalcophile elements*

248   The stainless steels used in the lunar curatorial facility contain a range of slightly (SSE),

249   moderately siderophile elements (MSE), and highly chalcophile elements (HCE). These elements,

250   which include Cr (SSE), Mo, W (MSE) and Se (HCE) are of significant interest, both for isotopic

251   tracing of materials (e.g., Warren, 2011; Kruijer et al., 2015) and for investigating volatile-

252   siderophile element delivery to the Moon (e.g., Wang & Becker, 2013). While the Cr, Mo and W

253   isotopic compositions of the stainless steels should ultimately be determined by interested parties,

254   we note the magnitude of element addition possible at low mass addition (~0.1%) is generally

255   minor (~100 $\mu g\ g^{-1}$ Cr, ~30 $\mu g\ g^{-1}$ Cu, <1 $\mu g\ g^{-1}$ Mo, <0.2 $\mu g\ g^{-1}$ W, ~0.003 $\mu g\ g^{-1}$ Se; **Figure 3**).

256   The concentrations of SSE, MSE and HCE are high enough in the stainless steels, however, that

257   some key ratios used for investigating volatile processes (e.g., Cu/Ag or Se/Te) might be affected,

258   as would some lunar rocks that have low Cu, Se, Mo or W contents.

259

260   Given that terrestrial metal is likely to have 'normal' isotopic compositions of Cr, Mo, and

261   W, the magnitude of effect on original isotopic composition assuming, at most, 0.1% mass addition

262   would be quite limited. For example, both Touboul et al. (2015) and Kruijer et al. (2015) note

263   small [182]W excess (~21-28 ppm) measured in lunar rocks, compared to the silicate Earth, consistent

264   with disproportional late accretion, as also inferred from the HSE (Day et al., 2007; Day & Walker,

265   2015). To generate a shift of this magnitude, from metal contamination alone, would require up to

266   10% by mass contamination of a metal with $^{182}W/^{184}W$ characteristics like early-formed, Hf-

267 depleted planetesimal iron cores (e.g., Horan et al., 1998). As noted for the HSE, this amount of

268 mass addition during curatorial processing is highly unlikely and would be visually detectable.

269

270 *4.3 Other possible sources of contamination for Apollo lunar samples*

271 In this study, we considered the effects of metal contamination during the curation and

272 processing of the Apollo samples at NASA Johnson Space Center. Despite the painstaking and

273 careful approach taken by astronauts and curatorial staff, since their collection on the Moon, the

274 Apollo samples have been subjected to a range of collection, curatorial and processing materials.

275 From the outset, during collection, the samples were taken from the conditions of collection into

276 lunar modules, where the indium edges on the sample container boxes did not remain hermetically

277 sealed. They have been preserved in terrestrial N_2 gas, within stainless steel boxes or containers,

278 wrapped in Teflon. The samples experienced exposure to magnetic fields, affecting both

279 acquisition of isothermal and viscous remnant magnetization (Pearce et al., 1974). Many of the

280 samples have also been sawn with diamond blade materials, which can heat samples and have

281 magnetic as well as chemical contamination effects. Our results confirm that, for metal, typically

282 significant physical addition (>0.1% by mass) of terrestrial materials would need to occur to have

283 a strong measurable effect on HSE, MSE, SSE or HCE in the Apollo samples. The only area of

284 curatorial processing where we have not done a detailed investigation is during cutting of the

285 Apollo samples at the NASA curatorial facility, including the use of saw blades, bands and wires

286 for wire saws. Saw blade material has been recognized on some lunar sample materials previously,

287 and the composition of the metal smears ($Fe_{0.75}Ni_{0.05}Cr_{0.15}$; Tikoo et al., 2014) is similar in

288 composition to the stainless-steel implements reported here. Nonetheless, the exact compositions

289 of these materials that could potentially contaminate the samples should ultimately be assessed.

290 Overall, we consider the likelihood of significant contamination of lunar samples during curation

291 and curatorial processing for most elements by metal contamination to be low.

292

293 **Conclusions**

294 Our results imply a generally negligible contribution from metal contamination during

295 curation and sample processing in the NASA Johnson Space Center curatorial facility. While

296 further work to constrain contamination on other properties of Apollo samples is required (e.g.,

297 magnetics, organics, anaerobic microbes, water, nitrogen, noble gases), the effect of metal

298   contamination can be constrained for the Apollo lunar collection. Our results do not preclude

299   contamination effects from saw-blades or from the handling of samples by lunar principal

300   investigators after they have received samples.

301

309

310   **References**

311   Allen C, Allton J, Lofgren G, Righter K, Zolensky M (2011) Curating NASA's extraterrestrial

312   samples – past, present and future. Chem der Erde 71, 1-20

313   Allton JH, Bagby JR Jr, Stabekis PD (1998) Lessons learned during Apollo lunar sample

314   quarantine and sample curation. Adv. Space Res. 22, 373-382

315   Burkhardt C, Hin RC, Kleine T, Bourdon B (2014) Evidence for Mo isotope fractionation in the

316   solar nebula and during planetary differentiation. Earth Planet Sci Lett 391, 201-211

317   Cook DL, Walker RJ, Horan MF, Wasson JT, Morgan JW (2004) Pt-Re-Os systematics of group

318   IIAB and IIIAB iron meteorites. Geochimica et Cosmochimica Acta 68, 1413-1431

319   Day JMD (2013) Hotspot volcanism and highly siderophile elements. Chemical Geology 341, 50-

320   74

321   Day JMD, Walker RJ (2015) Highly siderophile element depletion in the Moon. Earth and

322   Planetary Science Letters 423, 114-124

323   Day JMD, Pearson DG, Taylor LA (2007) Highly siderophile element constraints on accretion and

324   differentiation of the Earth-Moon system. Science 315, 217-219

325   Day JMD, Walker RJ, James OB, Puchtel IS (2010) Osmium isotope and highly siderophile

326   element systematics of the lunar crust. Earth and Planetary Science Letters 289, 595-605

327   Day JMD, Brandon AD, Walker RJ (2016) Highly Siderophile Elements in Earth, Mars, the Moon,

328   and Asteroids. Reviews in Mineralogy and Geochemistry 81, 161-238

329   Day JMD, Waters CL, Schaefer BF, Walker RJ, Turner S (2016b) Use of Hydrofluoric Acid

330   Desilicification in the Determination of Highly Siderophile Element Abundances and Re-Pt-Os

331   Isotope Systematics in Mafic-Ultramafic Rocks. Geostandards and Geoanalytical Research 40,

332   49-65

333   Day, JMD, Moynier F, Shearer CK (2017) Late-stage magmatic outgassing from a volatile-

334   depleted Moon. Proceedings of the National Academy of Sciences 114, 9547-9551

335   Fischer-Gödde M, Becker H (2012) Osmium isotope and highly siderophile element constraints

336   on ages and nature of meteoritic components in ancient lunar impact rocks. Geochimica et

337   Cosmochimica Acta 77, 135-156

338   Fischer-Gödde M, Becker H, Wombacher F (2010) Rhodium, gold and other highly siderophile

339   element abundances in chondritic meteorites. Geochimica et Cosmochimica Acta 74, 356-379

340   Gleißner P, Becker H (2017) Formation of Apollo 16 impactites and the composition of late

341   accreted material: Constraints from Os isotopes, highly siderophile elements and sulfur

342   abundances. Geochemica et Cosmochimica Acta 200, 1-24

343   Hertogen J, Janssens M-J, Takahashi H, Palme H, Anders E (1977) Lunar basins and craters:

344   Evidence for systematic compositional changes of bombarding population. Proc. Lunar. Sci.

345   Conf. 8th, 17-45

346   Higuchi H, Morgan JW (1975) Ancient meteoritic component in Apollo 17 boulders. Proc. Lunar

347   Sci. Conf. 6th, 1625-1651

348   Horan MF, Smoliar M, Walker RJ (1998) ^{182}W and ^{187}Re-^{187}Os systematics of iron meteorites:

349   chronology for melting, differentiation and crystallization of asteroids. Geochimica et

350   Cosmochimica Acta 62, 545-554

351   Horan MF, Walker RJ, Morgan JW, Grossman JN, Rubin A (2003) Highly siderophile elements

352   in chondrites. Chemical Geology 196, 5-20

353   Korotev RL (1994) Compositional variation in Apollo 16 impact-melt breccias and inferences for

354   the geology and bombardment history of the Central Highlands of the Moon. Geochim.

355   Cosmochim. Acta 58, 3931-3969

356   Kruijer T, Kleine T, Fischer-Gödde M, Sprung P (2015) Lunar tungsten isotopic evidence for the

357   late veneer. Nature, 520, 534-537

358   Liu J, Sharp M, Ash RD, Kring DA, Walker RJ (2015). Diverse impactors in Apollo 15 and 16
359   impact melt rocks: evidence from osmium isotopes and highly siderophile elements.
360   Geochimica et Cosmochimica Acta 155, 122-153

361   McCoy TJ, Walker RJ, Goldstein JI, Yang J, McDonough WF, Rumble D, Chabot NL, Ash RD,
362   Corrigan CM, Michael JR, Kotula PG (2011) Group IVA irons: new constraints on the
363   crystallization and cooling history of an asteroidal core with a complex history. Geochim.
364   Cosmochim. Acta 75, 6821-6843

365   Norman MD, Bennett VC, Ryder G (2002) Targeting the impactors: siderophile element signatures
366   of lunar impact melts from Serenatatis. Earth and Planetary Science Letters, 202, 217-228

367   Papanastassiou D, Day JMD, Glavin DP, Huss GR., Korotev RL, Nyquist LE, Wadhwa M, Zega
368   TJ (2015) Lunar Curation Task Force Report. NASA report to the Curation and Analysis
369   Planning Team for Extraterrestrial Materials, 14pp.

370   Pearce GW, Gose WA, Strangway DW (1974) Magnetic studies of Apollo 15 and 16 lunar
371   samples. Proceedings of the fourth lunar science conference 3, 3045-3076

372   Petaev MI, Jacobsen SB (2004) Differentiation of metal-rich meteoritic parent bodies: I.
373   Measurements of PGEs, Re, Mo, W, and Au in meteoritic Fe-Ni metal. Meteoritics and
374   Planetary Science, 39, 1685-1697

375   Puchtel IS, Walker RJ, James OB, Kring DA (2008) Osmium isotope and highly siderophile
376   element systematics of lunar impact melt rocks: Implications for the late accretion history of
377   the Moon and Earth. Geochim. Cosmochim. Acta 72, 3022-3042

378   Sharp M, Gerasimenko I, Loudin L, Liu J, James OB, Puchtel IS, Walker RJ (2014)
379   Characterization of the dominant impactor signature for Apollo 17 impact melt rocks.
380   Geochimica et Cosmochimica Acta 131, 62-80

381   Smoliar MI, Walker RJ, Morgan JW (1996) Re-Os ages of group IIA, IIIA, IVA and IVB iron
382   meteorites. Science 271, 1099-1102

383   Tikoo SM, Weiss BP, Cassata WS, Shuster DL, Gattacceca J, Lima EA, Suavet C, Nimmo F,
384   Fuller MD (2014) Decline of the lunar core dynamo. Earth and Planetary Science Letters 404,
385   89-97

386   Touboul M, Puchtel IS, Walker RJ (2015) Tungsten isotopic evidence for disproportional late
387   accretion to the Earth and Moon. Nature, 520, 530-533

388   Verchovsky AB, Mortimer J, Buikin AI, Anand M (2017) Trapping of atmospheric gases during
389   crushing of lunar sample. Lunar and Planetary Science Conference, XLVIII, 2204.
390   Walker RJ, Horan MF, Shearer CK, Papike JJ (2004) Depletion of highly siderophile elements in
391   the lunar mantle: evidence for prolonged late accretion. Earth and Planetary Science Letters
392   224, 399-413
393   Walker RJ, McDonough WF, Honesto J, Chabot NL, McCoy TJ, Ash RD, Bellucci JJ (2008)
394   Modeling fractional crystallization of group IVB iron meteorites. Geochimica et Cosmochimica
395   Acta 72, 2198-2216
396   Wang Z, Becker H (2013) Ratios of S, Se and Te in the silicate Earth require a volatile-rich late
397   veneer. Nature 499, 328-331
398   Warren PH (2011) Stable-isotopic anomalies and the accretionary assemblage of the Earth and
399   Mars: A subordinate role for carbonaceous chondrites. Earth and Planetary Science Letters 311,
400   93-100

401   **Figures and Figure Captions**

402

403   **Figure 1:** Images of tools, sample containers and other metal curation devices used during Apollo
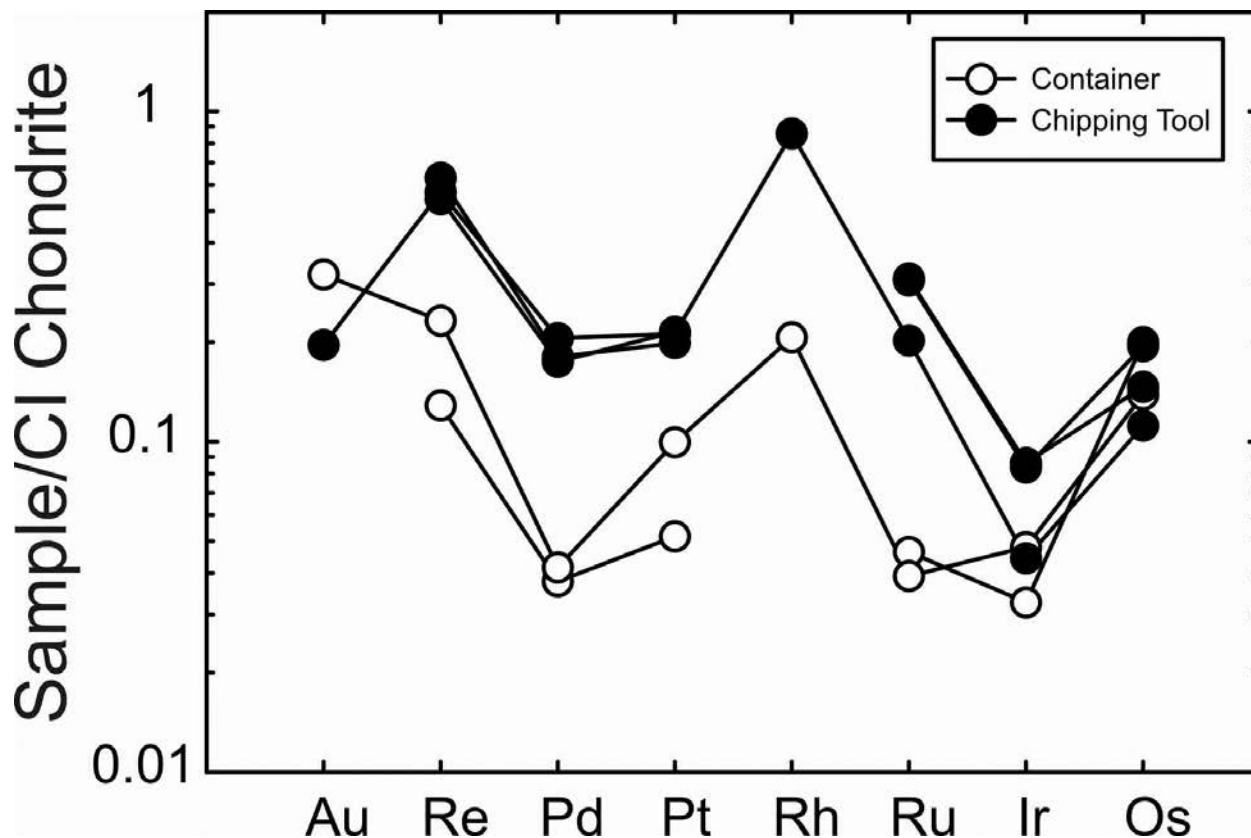
404   sample preparation.

405

406

407

408   **Figure 2:** CI-chondrite normalized highly siderophile element patterns for NASA stainless steel

409   curational materials, measured by isotope dilution TIMS/ICP-MS and LA-ICP-MS. CI-chondrite

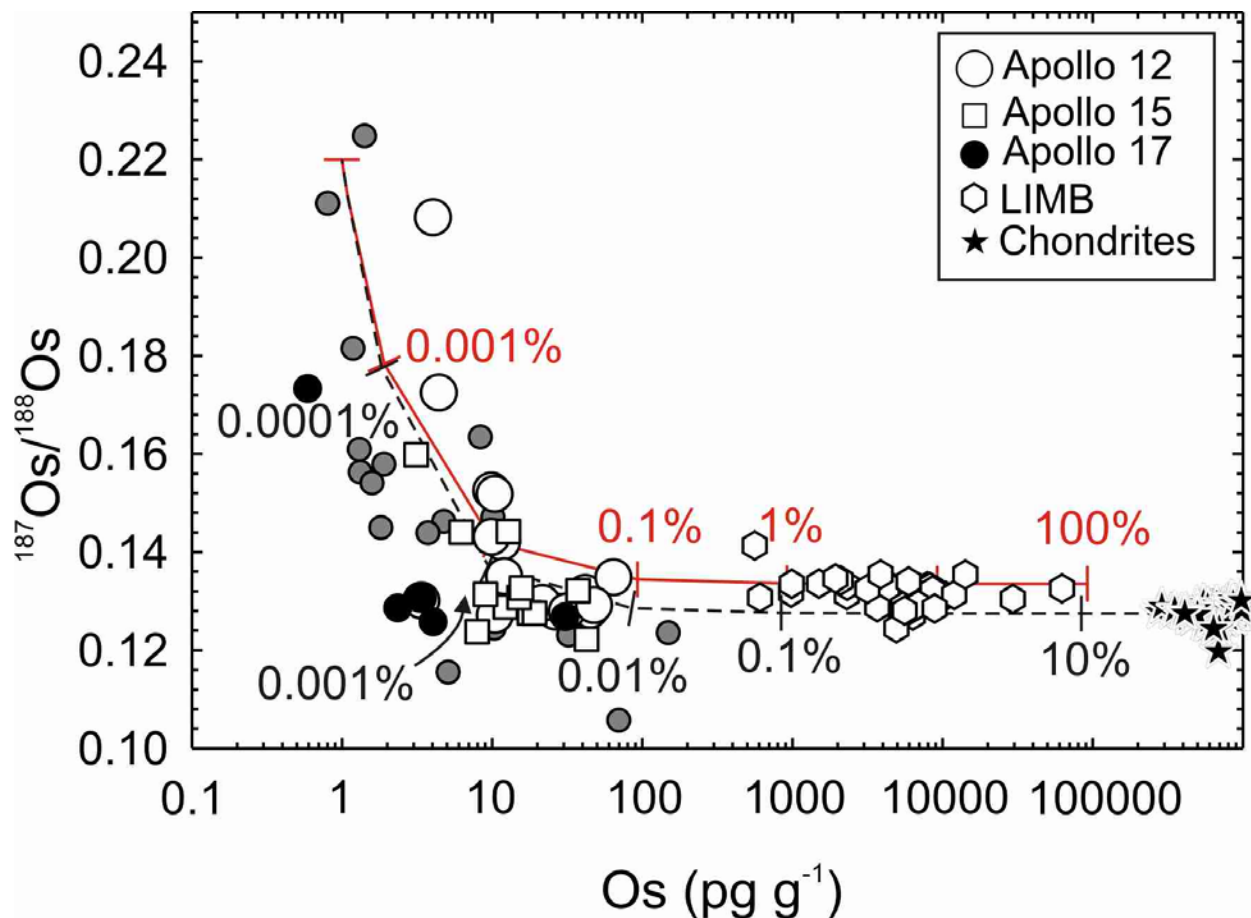410   normalization from the compilation in Day et al. (2016).

411

412

Figure 3: Osmium concentration (pg g^{-1}) versus $^{187}Os/^{188}Os$ for Apollo 12, 15 and 17 lunar mare basalts (Day et al., 2007; Day & Walker, 2015), lunar pristine crustal rocks (Day et al., 2010; grey filled circles), lunar impact-melt breccias (LIMB; e.g., Puchtel et al., 2008; Fischer-Godde & Becker, 2012), and ordinary, carbonaceous, enstatite and rumuruti chondrites (Horan et al., 2003; Fischer-Godde et al., 2010). The solid curve shows mixing between a hypothetical mare basalt parental melt composition, from Day & Walker (2015), with very low Os ($^{187}Os/^{188}Os$ - ~0.22; Os = 1 pg g^{-1}), and the NASA curatorial Type 304 stainless steel ($^{187}Os/^{188}Os$ - 0.1336; Os = 92,100 pg g^{-1}). The dashed curve shows mixing between the hypothetical mare basalt parental melt and an averaged chondritic contaminant ($^{187}Os/^{188}Os$ = 0.127; Os = 600,000 pg g^{-1}). Percentages (by mass) of the various components along the mixing lines are labelled.
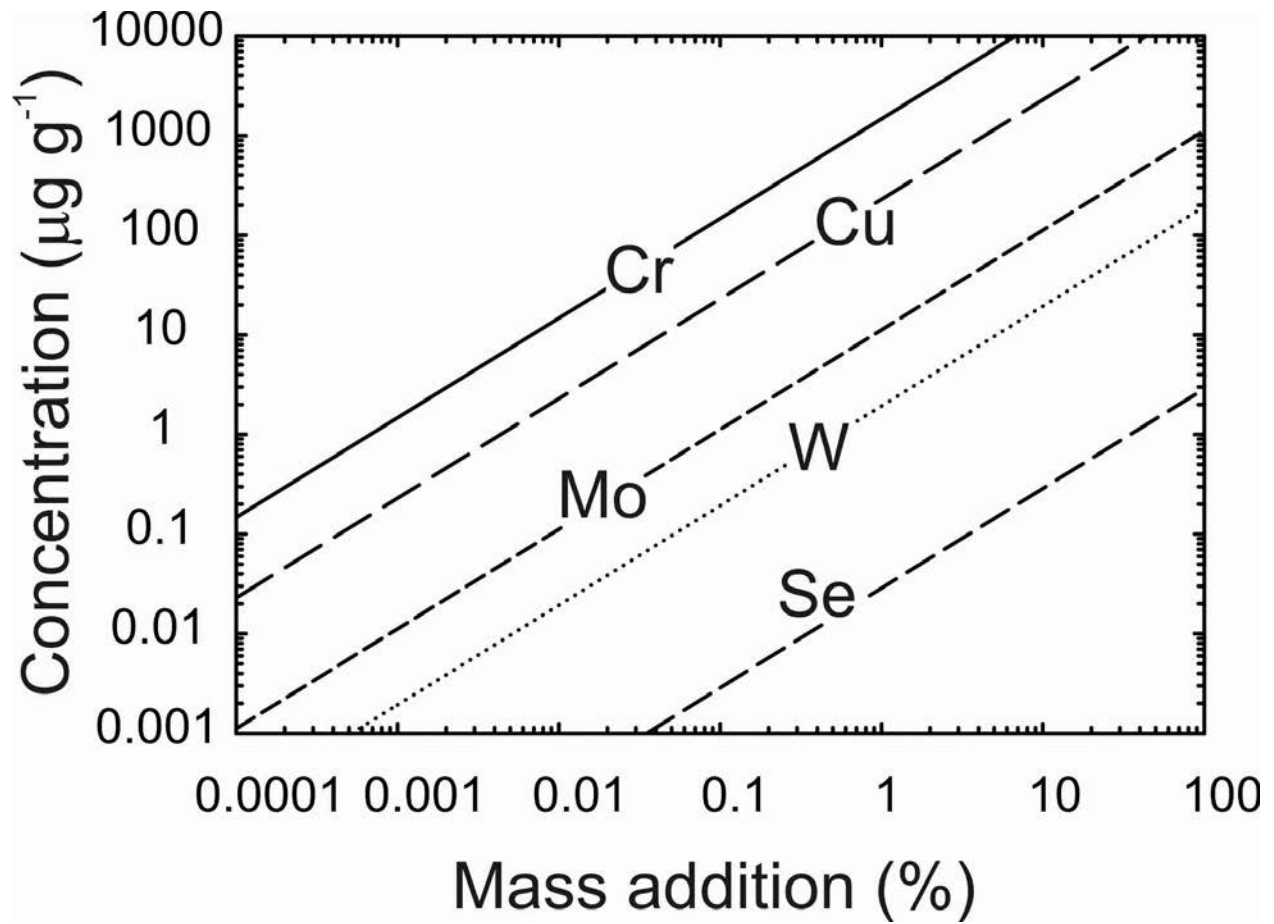
423
424
425 **Figure 4:** Concentration of an element added to a sample as a function of physical mass addition
426 for Se, W, Mo, Cu and Cr for lunar curational stainless steels.

427

428

429

430